Resonance energy transfer: The unified theory revisited

Gareth J. Daniels, Robert D. Jenkins, David S. Bradshaw, and David L. Andrews

Citation: The Journal of Chemical Physics **119**, 2264 (2003); doi: 10.1063/1.1579677

View online: http://dx.doi.org/10.1063/1.1579677

View Table of Contents: http://scitation.aip.org/content/aip/journal/jcp/119/4?ver=pdfcov

Published by the AIP Publishing

Resonance energy transfer: The unified theory revisited

Gareth J. Daniels, Robert D. Jenkins, David S. Bradshaw, and David L. Andrews[a)]
School of Chemical Sciences and Pharmacy, University of East Anglia, Norwich NR4 7TJ, United Kingdom

(Received 4 March 2003; accepted 14 April 2003)

Resonance energy transfer (RET) is the principal mechanism for the intermolecular or intramolecular redistribution of electronic energy following molecular excitation. In terms of fundamental quantum interactions, the process is properly described in terms of a virtual photon transit between the pre-excited donor and a lower energy (usually ground-state) acceptor. The detailed quantum amplitude for RET is calculated by molecular quantum electrodynamical techniques with the observable, the transfer rate, derived *via* application of the Fermi golden rule. In the treatment reported here, recently devised state-sequence techniques and a novel calculational protocol is applied to RET and shown to circumvent problems associated with the usual method. The second-rank tensor describing virtual photon behavior evolves from a Green's function solution to the Helmholtz equation, and special functions are employed to realize the coupling tensor. The method is used to derive a new result for energy transfer systems sensitive to both magnetic- and electric-dipole transitions. The ensuing result is compared to that of pure electric-dipole–electric-dipole coupling and is analyzed with regard to acceptable transfer separations. Systems are proposed where the electric-dipole–magnetic-dipole term is the leading contribution to the overall rate. © *2003 American Institute of Physics.* [DOI: 10.1063/1.1579677]

I. INTRODUCTION

In numerous photosensitive systems, resonance energy transfer (RET) mediates a redistribution of electronic energy following UV/visible excitation. Fundamentally the same mechanism effects the migration of excitation energy from pre-excited donors to suitable acceptors across a host of these chemically different systems—in which the constituents may comprise individual molecules, ions or chromophore sites in biomolecular and other macromolecular assemblies. RET is a key phenomenon observed in natural light-harvesting complexes, accounting for energy hopping between chlorophyll molecules in the photosynthetic unit (PSU)[1–5]—and thereby representing an essential component of life chemistry. In such complex, naturally occurring systems, it has become possible to determine the detailed molecular structures. For example, studies on bacterial photosystems have elucidated the structures for reaction centers in *Rhodopseudomonas* (*Rps.*) *viridis*,[6] the peripheral light-harvesting complex of *Rps. acidophila*,[7,8] and the Fenna–Matthews–Olson protein complex in the green sulphur bacterium *Prosthecochloris aestuarii*.[9] In the case of higher plants and algae there have also been notable successes in determining the light-harvesting complexes and chlorophyll arrangement in Photosystem I.[10–12] These investigations, amongst others, are proving useful for *in vivo* investigations—and also for the informed development of detailed molecular models for photobiology.

The structural elucidation of key components in many photosynthetic systems has been timely for the development of synthetic light-harvesting analogues. Modern pulsed laser techniques have afforded a detailed characterization of the energy hopping dynamics in several such systems designed to mimic biological antenna complexes.[13–15] This area represents a benchmark for research into systems exhibiting RET, and already a striking success has been reported in the creation of a complete artificial photosystem.[16] At a lower level of molecular complexity, relatively simple bichromophore, donor–acceptor molecules provide environments within which energy migration is readily observed; such molecules have been the subject of a number of reviews.[17–19] Notable amongst more complex, multichromophore systems are cyclodextrins[20,21] and other multiporphyrin arrays.[22–24] Dendrimers also feature prominently in recent research; these highly branched macromolecules comprise chromophores linked in fractal or other highly symmetric geometries[25] and much interest has focused upon energy transfer from their dendritic constituents to photoactive cores.[26] Dendrimers display a variety of photophysical effects resulting from intramolecular resonance energy transfer, including photoisomerization,[27,28] light-harvesting,[29,30] and directed energy transfer or funneling.[31] The high symmetry of many such multichromophore arrays offers new investigative routes and recent research has demonstrated preferential channeling involving exciton states.[32]

Although scrutiny of the role of resonance energy transfer is most acute in connection with photosynthesis and energy harvesting, this by no means circumscribes other applications. For example, the popularly termed ''spectroscopic ruler'' (fluorescence resonance energy transfer, FRET[33,34]), which delivers information on intramolecular distances based on application of the basic equations of RET, is now routinely used as an adjunct in protein structure determination. RET is also observed in such diverse materials as levitated microdroplets,[35] lanthanide-doped lattices,[36] conjugated polymer chains[37] and both interlayer and intralayer transfer

a)Electronic mail: d.l.andrews@uea.ac.uk

in Langmuir–Blodgett (LB) films[38–40]—and it has recently been linked with vibrational energy redistribution in water.[41] A wealth of diverse information can be ascertained from analysis of such processes; in LB-films alone, their study has afforded new insights into interlayer structures,[42,43] modified transfer dynamics in restricted geometries,[44,45] and both substrate[46,47] and micellar/surfactant effects.[48] Against the backdrop of intense research and development it is timely to revisit the theory which describes this fundamental pairwise (donor–acceptor) interaction.

Over subnanometer distances, donor–acceptor energy transfer commonly displays a rate characterized by a negative exponential dependence on the pair separation. Attributed to an *electron exchange* involving wave function overlap, this mechanism was first formulated by Dexter in the 1950s to account for the phenomenon of sensitized luminescence.[49] In its connection with special cases of electronically associated multichromophore systems the exchange mechanism has more recently been the subject of much discussion by Scholes, Ghiggino and co-workers.[50–54] Our concern is with energy transfer between electronically independent donor–acceptor moieties, beyond significant wave function overlap. Until the late 1980s, when a resurgence of interest culminated in a fresh development of theory, such RET was widely considered to proceed by one of two distinct mechanisms. In the short-range (nanoscale separation regime) a *radiationless* transfer mechanism exhibiting an inverse sixth power distance dependence was deduced by the eponymous *Förster*.[55] In the long-range (pair separations exceeding optical wavelengths) a *radiative*, photon emission-capture process yielding the familiar inverse square law was thought to operate[56]—the latter mechanism attested by the reabsorption of photons in optically thick samples.[57] In a *unified theory* formulated by Andrews and co-workers in a series of works[58–60] the radiationless and radiative mechanisms were identified as the short- and long-range asymptotes of a single mechanism. Based on quantum electrodynamics (QED), and following ground-breaking quantum mechanical work by Avery[56] and Gomberoff and Power,[61] the unified theory establishes energy transfer as a process mediated by the propagation of *virtual photons*, optical quanta whose character becomes progressively ''real'' and energy conserving as their propagation distance (and hence lifetime) increases.

It is the main purpose of this work to explore difficulties and alternative calculational strategies in the quantum treatment, and to extend the theory by full inclusion of magnetic-dipole interactions. The analysis begins in Section II with a synopsis of the development behind RET theory and its formulation in the framework of molecular QED; RET is then reappraised from a contemporary viewpoint utilizing a recently formulated state-sequence technique. By developing the quantum amplitude in terms of a Green's function, it is shown how different approaches to the ensuing calculations can lead to divergences in the final results. In Sec. III the standard residue theorem and boundary condition approach to the Green's function calculation is presented and deconstructed. A new method is then introduced and shown to obviate significant problems related to the residue theorem technique. It is also shown that it is unnecessary to fully restrict the results by classical arguments and that a single equation can accommodate both mathematical and experimental rigors. In Sec. IV, the new method is applied to RET engaging both magnetic and electric transition dipoles. Similar problems to those noted in Sec. III are identified and a means found for their circumvention. Finally, in Sec. V, the overall rate of energy transfer including both magnetic and electric effects is analyzed. Each term is examined and situations are discussed where electric–magnetic coupling provides the leading rate contribution.

II. THEORY

The fundamental process of RET, in a donor–acceptor *interaction-pair AB*, may be represented by the simple nonchemical equation;

$$A^{\alpha}+B^{0}\xrightarrow{\text{RET}}A^{0}+B^{\beta}. \tag{2.1}$$

Here, superscripts denote donor and acceptor states, greek letters indicating the relevant electronic excited states and 0 the ground state. Equation (2.1) does not depict a conventional chemical reaction and *only* illustrates electronic states before and after RET. In the unified theory description, the coupling of donor and acceptor transitions is mediated by the propagation of a virtual photon. These messenger particles cannot be directly detected; in this respect the virtual photon assumes a role similar to that of virtual electronic states involved in scattering processes.[62] The virtual photon formulation entails summation over all possible wave-vectors and polarizations, just as virtual molecular states invoke a summation over energy levels. At relatively small interaction-pair separations (those within normal Förster limits) photon time of flight is short and a large uncertainty in the system energy is present. However, as the interaction-pair separate this uncertainty is reduced, effectively imposing on the virtual photon an increasingly real character until (in the regime of radiative transfer) virtual traits become indiscernible. In principle even seemingly pure radiative photons retain some virtual character associated with time-energy uncertainty. ''In a sense every photon is virtual, being emitted and then sooner or later being absorbed.''[63] In the unified theory this behavior is seamlessly accommodated into a single, very simple but all-encompassing rate equation.[59]

A. Molecular QED formalism

Recent developments in the tools of molecular quantum electrodynamics have led to a more accurate depiction of virtual photon behavior. No process involving virtual states can adequately be represented using energy level diagrams, as is well known. However the time-ordered diagrams conventionally adopted for such purposes, constructed from world-line segments and departure/arrival conjunctions, fail to meaningfully represent the virtual photon coupling of an interaction-pair. The messenger has indefinite wave-vector, for example, and in this alone the pictorial representation is incorrect. Moreover the associated machinery becomes enormously cumbersome when applied to more complex, intricately coupled energy pooling systems.[64] A very recently de-

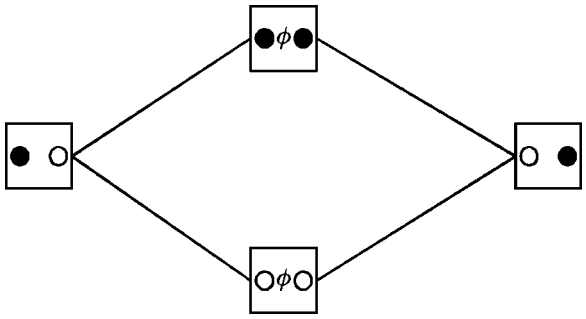

FIG. 1. State-sequence diagram for resonance energy transfer, donor A is represented by the circle on the left of each box, B the circle on the right. Shaded circles show a ground state species in the excited state; other circles represent a species; ϕ depicts a virtual photon.

veloped hyperspace description of molecular QED circumvents these and other problems—not only in connection with energy transfer and associated multiphoton processes but also nonlinear optics—and it is this approach which is adopted hereafter.[65]

In the hyperspace representation, every process is first categorized in terms of the number of matter-radiation interactions it entails; RET is described by the state-sequence diagram of Fig. 1 (see Ref. 65 for a full explanation). Tracing the lower pathway; the virtual photon (its presence in the system symbolized by ϕ) is created at A and annihilated at B. The upper path depicts the case where ϕ is created at B and annihilated at A (see figure legend), as is also consistent with the time-energy uncertainty basis for conventional time orderings. As both paths lead to the same final, isoenergetic state, calculation of the full RET quantum amplitude requires their summation. Even though the lower pathway contribution becomes overwhelmingly dominant as interaction-pair separation increases, the upper pathway can never be entirely discounted. In this respect, to envisage the virtual photon only departing from A and arriving at B sanctions an unjustified semantic prejudice—as it excludes the latter mechanism. As RET is essentially the relocation of electronic excitation energy within an interaction-pair, *both* time orderings shown in Fig. 1 are involved. Although it is not our concern here, the causality of energy transfer is also of considerable interest,[66,67] while other ongoing work is affording a detailed quantification of the relative contributions of each path to the overall rate result.[68]

In Fig. 1 all states are represented by system-state boxes which exemplify products of matter and radiation states. A general state $|r_k^m\rangle$ may be represented as

$$|r_k^m\rangle=\prod_{\xi}\ |\xi^{r_k^m}\rangle|\mathrm{rad}_{r_k^m}\rangle\equiv|\mathrm{mat}_{r_k^m}\rangle|\mathrm{rad}_{r_k^m}\rangle\equiv|\mathrm{mat}_{r_k^m};\mathrm{rad}_{r_k^m}\rangle, \tag{2.2}$$

where k is the number of steps across the state-sequence diagram, and m is a state label.[63] The state of (2.2) follows the detailed notation introduced in Ref. 65 and is used here in this elementary case to introduce concepts which prove to greatly simplify calculations involved in higher-order cases. The matter constituent of (2.2) entails a product of the relevant electronic states $\xi^{r_k^m}$ of all participating species ξ. The energy of $|r_k^m\rangle$, $E_{r_k^m}$, comprises a sum of radiation and matter energies—the latter a sum of contributions from all participant species, $E^{\xi}_{r_k^m}$. Using the notation of (2.2) the isoenergetic initial and final states, now denoted by $|r_0^1\rangle$ and $|r_2^1\rangle$ respectively, can be written as

$$|r_0^1\rangle=|A^{\alpha}B^0;0(\mathbf{p},\lambda)\rangle \tag{2.3}$$

and

$$|r_2^1\rangle=|A^0B^{\beta};0(\mathbf{p},\lambda)\rangle. \tag{2.4}$$

Note that the photon occupation number of the radiation state is zero; the virtual photon with integration-variable wave-vector $\mathbf{p}$ and polarization λ is not present in the initial or final system-states since both are of effectively infinite lifetime and thus have no energy uncertainty. Given that $E_{r_0^1}=E_{\alpha}^A+E_0^B$ and $E_{r_2^1}=E_0^A+E_{\beta}^B$, the important energy identity

$$E_{\alpha 0}^A=E_{\beta 0}^B=\hbar ck \tag{2.5}$$

follows, where $\hbar ck$ is the total transferred energy and $E^{\xi}_{r_k^m(r_k^m)'}=E^{\xi}_{r_k^m}-E^{\xi}_{(r_k^m)'}$. Returning to Fig. 1, the lower route, where virtual photon creation occurs at A, produces a virtual system-state characterized by a state-sequence box representing the ket $|r_1^1\rangle=|A^0B^0;1(\mathbf{p},\lambda)\rangle$ and energy $E_{r_1^1}=E_0^A+E_0^B+\hbar cp$. Similarly the upper path, where virtual photon creation occurs at B, elicits the state-sequence box representing the ket $|r_1^2\rangle=|A^{\alpha}B^{\beta};1(\mathbf{p},\lambda)\rangle$ and energy $E_{r_1^2}=E_{\alpha}^A+E_{\beta}^B+\hbar cp$.

As the total number of matter-radiation interactions in RET is 2, the quantum amplitude, M_{fi}, is calculated from the second term of an expansion in time-dependent perturbation theory. Explicitly

$$M_{fi}=\sum_{m=1}^{2}\ \frac{\langle r_2^1|H_{\mathrm{int}}|r_1^m\rangle\langle r_1^m|H_{\mathrm{int}}|r_0^1\rangle}{E_{r_0^1}-E_{r_1^m}} \tag{2.6}$$

which introduces the interaction Hamiltonian H_{int} given by

$$H_{\mathrm{int}}=-\varepsilon_0^{-1}\sum_{\xi}\ \boldsymbol{\mu}(\xi)\cdot\mathbf{d}^{\perp}(\mathbf{R}_{\xi}) \tag{2.7}$$

in the electric-dipole approximation. Present in expression (2.7) are two operators; the electric-dipole moment operator $\boldsymbol{\mu}(\xi)$ operating on molecular states $|\xi^{r_k^m}\rangle$ and the transverse electric field displacement operator $\mathbf{d}^{\perp}(\mathbf{R}_{\xi})$ operating on $|\mathrm{rad}_{r_k^m}\rangle$. The latter, evaluated for the position of ξ $(\mathbf{R}_{\xi})$, is usually written as the mode expansion

$$\mathbf{d}^{\perp}(\mathbf{R}_{\xi})=\mathrm{i}\sum_{\mathbf{p},\lambda}\left(\frac{\varepsilon_0\hbar cp}{2V}\right)^{\frac{1}{2}}\{\mathbf{e}^{(\lambda)}(\mathbf{p})a^{(\lambda)}(\mathbf{p})\mathrm{e}^{\mathrm{i}\mathbf{p}\cdot\mathbf{R}_{\xi}}-\overline{\mathbf{e}}^{(\lambda)}(\mathbf{p})a^{\dagger(\lambda)}(\ \mathbf{p})e^{-\mathrm{i}\mathbf{p}\cdot\mathbf{R}_{\xi}}\}, \tag{2.8}$$

where $\mathbf{e}^{(\lambda)}(\mathbf{p})$ is the polarization vector of a virtual photon ϕ with wave-vector $\mathbf{p}$ and polarization λ, $\overline{\mathbf{e}}^{(\lambda)}(\mathbf{p})$ being its complex conjugate; $a^{(\lambda)}(\mathbf{p})$ and $a^{\dagger(\lambda)}(\mathbf{p})$ respectively are annihilation and creation operators for ϕ, and V is an arbitrary quantization volume. The vacuum form of $\mathbf{d}^{\perp}(\mathbf{R}_{\xi})$ used for

present purposes does not directly engage media effects, their inclusion here obscuring the key emergent issues. Nonetheless it should be noted that extensive effort has been undertaken to develop a theory encompassing the electronic effects of any intervening medium.[69–72] A straightforward prescriptive approach to the modification required by this formulation is described elsewhere[73] and may easily be applied to the results obtained below.

Recognizing the states and energies introduced earlier, for electric-dipole–electric-dipole (e–e) resonance energy transfer M_{fi}^{e-e}, (2.6) becomes;

$$M_{fi}^{e-e}=\frac{\langle r_2^1|H_{\rm int}|r_1^1\rangle\langle r_1^1|H_{\rm int}|r_0^1\rangle}{(E_{r_0^1}-E_{r_1^1})}+\frac{\langle r_2^1|H_{\rm int}|r_1^2\rangle\langle r_1^2|H_{\rm int}|r_0^1\rangle}{(E_{r_0^1}-E_{r_1^2})}, \tag{2.9}$$

where the first and second terms embody the upper and lower paths of Fig. 1, respectively. By the application of Eqs. (2.5), (2.7), and (2.8), on (2.9),

$$M_{fi}^{e-e}=(2\varepsilon_0 V)^{-1}\sum_{\mathbf{p},\lambda} p\overline{e}_i^{(\lambda)}(\mathbf{p})e_j^{(\lambda)}(\mathbf{p})\times\left\{\frac{\mu_i^{0\alpha(A)}\mu_j^{\beta 0(B)}e^{i\mathbf{p}\cdot\mathbf{R}}}{k-p}+\frac{\mu_j^{0\alpha(A)}\mu_i^{\beta 0(B)}e^{-i\mathbf{p}\cdot\mathbf{R}}}{-k-p}\right\}. \tag{2.10}$$

In the new notation $\boldsymbol{\mu}^{(r_k^m)'r_k^m}(\xi)=\langle\xi^{(r_k^m)'}|\boldsymbol{\mu}(\xi)|\xi^{r_k^m}\rangle$ is a transition dipole moment and $\mathbf{R}=\mathbf{R}_B-\mathbf{R}_A$ the intermolecular separation vector. Also the convention of summation over repeated Cartesian indices is implemented.

The wave-vector and polarization summations which need to be implemented in (2.10) can be achieved following the techniques of Craig and Thirunamachandran.[74] Extending the boundaries of the quantization volume we recognize that each lattice point in $\mathbf{p}$-space represents a realizable $\mathbf{p}$-vector and the wave-vector sum may be converted to an integral as $V\to\infty$

$$\frac{1}{V}\sum_{\mathbf{p}}\underset{\lim V\to\infty}{\Rightarrow}\int\frac{d^3\mathbf{p}}{(2\pi)^3}. \tag{2.11}$$

The polarization sum is tackled by using the sum rule

$$l_{i\alpha}l_{j\alpha}=\delta_{ij}, \tag{2.12}$$

where $l_{i\alpha}$ is the cosine of the angle between an axis in the laboratory frame (denoted by roman letters) and one in an independent frame (greek letters). Choosing the orthogonal frame set $\mathbf{e}^{(1)}(\mathbf{p})$, $\mathbf{e}^{(2)}(\mathbf{p})$ and $\mathbf{p}$ as the independent frame gives

$$e_i^{(1)}(\mathbf{p})\overline{e}_j^{(1)}(\mathbf{p})+e_i^{(2)}(\mathbf{p})\overline{e}_j^{(2)}(\mathbf{p})+\hat{p}_i\hat{p}_k=\delta_{ij}, \tag{2.13}$$

so that the polarization sum can be expressed as

$$\sum_{\lambda} e_i^{(\lambda)}(\mathbf{p})\overline{e}_j^{(\lambda)}(\mathbf{p})=\delta_{ij}-\hat{p}_i\hat{p}_j. \tag{2.14}$$

Implementing (2.11) and (2.14), M_{fi}^{e-e} is rewritten as

$$M_{fi}^{e-e}=\frac{\mu_i^{0\alpha(A)}\mu_j^{\beta 0(B)}}{2\varepsilon_0}\int p(\delta_{ij}-\hat{p}_i\hat{p}_j)\times\left\{\frac{e^{i\mathbf{p}\cdot\mathbf{R}}}{k-p}+\frac{e^{-i\mathbf{p}\cdot\mathbf{R}}}{-k-p}\right\}\frac{d^3\mathbf{p}}{(2\pi)^3}. \tag{2.15}$$

Converting this integral to spherical coordinates, $d^3\mathbf{p}\Rightarrow p^2\,dp\,d\Omega$ and with

$$-\int\hat{p}_i\hat{p}_j e^{\pm i\mathbf{p}\cdot\mathbf{R}}d\Omega=\frac{1}{p^2}\nabla_i\nabla_j\int e^{\pm i\mathbf{p}\cdot\mathbf{R}}d\Omega, \tag{2.16}$$

a change of variables allows (2.15) to be expressed as

$$M_{fi}^{e-e}=\frac{\mu_i^{0\alpha(\mathrm{A})}\mu_j^{\beta 0(\mathrm{B})}}{4\pi^2\varepsilon_0}(-\nabla^2\delta_{ij}+\nabla_i\nabla_j)\int_0^{2\pi}\int_{-1}^{1}\int_0^{\infty}\frac{p}{4\pi}\times\left\{\frac{e^{i\mathbf{p}\cdot\mathbf{R}}}{k-p}+\frac{e^{-i\mathbf{p}\cdot\mathbf{R}}}{-k-p}\right\}dp\,d(\cos\theta)d\phi. \tag{2.17}$$

Performing the angular integration gives

$$M_{fi}^{e-e}=\frac{\mu_i^{0\alpha(A)}\mu_j^{\beta 0(B)}}{2\pi^2\varepsilon_0}(-\nabla^2\delta_{ij}+\nabla_i\nabla_j)G(k,R), \tag{2.18}$$

introducing the Green's function $G(k,R)$ defined by

$$G(k,R)=\int_{-\infty}^{\infty}\frac{\sin pR}{2R}\left\{\frac{1}{k-p}+\frac{1}{-k-p}\right\}dp. \tag{2.19}$$

Various methods may be employed to resolve (2.19), and the following section reappraises the traditional (contour integration) methodology, highlighting its shortcomings and introducing a new method offering a solution to associated problems.

It is well known that $G(k,R)$ satisfies the Helmholtz equation

$$-(\nabla^2+k^2)G_k=\delta(\mathbf{R}), \tag{2.20}$$

where $G_k=G(k,R)$ and, as such, represents a link between classical and quantum thinking on wave propagation.[75] Upon first inspection, the Helmholtz equation delivers harmonic, $\mathbf{R}$-dependent solutions to the wave equation with the virtual photon wave-vector $\mathbf{p}$ adopting the role of the Helmholtz Fourier variable. However this conclusion relies upon the conceit of imposing the outgoing-wave (Sommerfeld radiation) boundary condition which ensures that the solution represents a physically realizable source, i.e., from initial conditions effectively localized in a finite region of space.[76] In both classical and semiclassical descriptions, envisaging a wavefront emanating from the donor offers a conceptually pleasing view of RET.[77] In QED however it is only the lower path of Fig. 1 (representing only one component of the quantum amplitude) that fits this model; it does not represent the behavior of the upper path. In the following it is shown that enforcing the Sommerfeld condition imposes a superfluous constraint and limitation on the QED form of the result.

III. ANALYSIS OF THE RET GREEN'S FUNCTION

We now present a juxtaposition of methods for solving Eq. (2.19). Previously tackled by use of the residue theorem

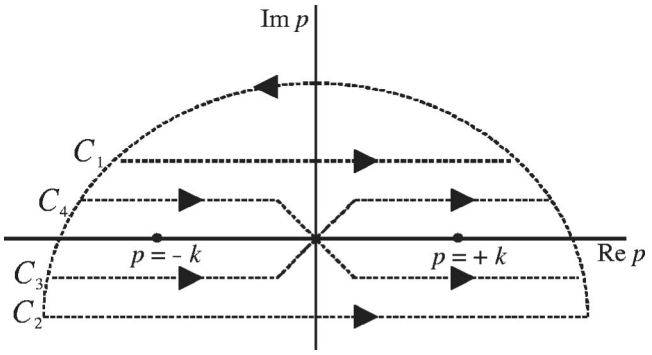

FIG. 2. Contours available for solution of the Green's function. All here are anticlockwise and closed in the upper imaginary plane.

and proving considerably problematic, here we introduce a new method based on the use of special functions which satisfactorily deals with the emergent issues.

A. Contour integration method

The solution of the Green's function (2.19), which exhibits poles at $p=\pm k$, is traditionally performed using the residue theorem. The choice of contour has been the subject of much discussion (*vide infra*). Conventionally two obvious choices present themselves: (i) to integrate using semicircles closed to infinity in the upper or lower complex planes, see Fig. 2; (ii) alternatively to shift the poles infinitesimally up or down and integrate along the real axis. Initial investigations by Craig and Thirunamachandran,[78] performed the integration on an anticlockwise contour C_2 closed in the upper complex plane. This identified the principal value as

$$G(k,R)=-\frac{\pi\cos kR}{R}. \tag{3.1}$$

Note that using clockwise contour C_1 closed in the lower complex plane yields an identical result. Taking the radiative limit ($kR\gg 1$) of (3.1), reveals an unverifiable $\cos^2 kR$ oscillation in the rate. Subsequent work by Andrews and Sherborne investigated the merits of all four possible integration contours illustrated in Fig. 2.[58] Closure of C_3 and C_4 in the upper complex plane gives further solutions which are complex conjugates of each other. The now generally accepted result, as chosen in Ref. 58, is that associated with C_4,

$$G(k,R)=-\frac{\pi}{R}e^{ikR}, \tag{3.2}$$

which satisfies the outgoing wave condition (though note that results from both C_3 and C_4 equally give correct behavior of the observable, which goes as the modulus squared of the quantum amplitude result). Equation (3.2) is the Green's function associated with a classical outgoing wave disturbance.[77]

Completion of the vector calculus in (2.18) on (3.2) results in an expression for the complete RET quantum amplitude expressible as

$$M_{fi}^{e-e}=\mu_i^{0\alpha(A)}V_{ij}(k,\mathbf{R})\mu_j^{\beta 0(B)}, \tag{3.3}$$

in which the dipole–dipole interaction is cast in terms of an intermolecular transfer tensor $V_{ij}(k,\mathbf{R})$. Explicitly this index-symmetric, fully retarded tensor is

$$V_{ij}(k,\mathbf{R})=\frac{e^{ikR}}{4\pi\varepsilon_0 R^3}\{(1-ikR)(\delta_{ij}-3\hat{R}_i\hat{R}_j) -k^2R^2(\delta_{ij}-\hat{R}_i\hat{R}_j)\}, \tag{3.4}$$

encompassing radiationless and radiative limits as its short- and long-range asymptotes, respectively. In the short-range (near-zone), this coupling tensor displays an R^{-3} distance dependence, though the terms linear and quadratic in kR increasingly modify the behavior as R increases. The term ''near-zone'' in practice indicates intermolecular distances below $R\approx 100$ Å (i.e., small compared to the characteristic optical distance k^{-1}) where the radiationless limit of energy transfer dominates. As R increases, retardation effects become more prominent and in the long-range limit, ($kR\gg 1$), Eq. (3.4) is dominated by the R^{-1} term, bringing the radiative mechanism to the fore. These are key features of the unified theory.

The transfer tensor $V_{ij}(k,\mathbf{R})$ can be decomposed into real and imaginary parts so that

$$V_{ij}(k,\mathbf{R})=\sigma_{ij}+i\tau_{ij}. \tag{3.5}$$

The real part, derived from C_2, is given by

$$\sigma_{ij}=(4\pi\varepsilon_0 R^3)^{-1}\{(\cos kR+kR\sin kR)(\delta_{ij}-3\hat{R}_i\hat{R}_j) -k^2R^2\cos kR(\delta_{ij}-\hat{R}_i\hat{R}_j)\}. \tag{3.6}$$

This is the result reported by Craig and Thirunamachandran which holds for the near-zone regime.[74] The imaginary part is revealed by the use of C_4,

$$\tau_{ij}=(4\pi\varepsilon_0 R^3)^{-1}\{(\sin kR-kR\cos kR)(\delta_{ij}-3\hat{R}_i\hat{R}_j) -k^2R^2\sin kR(\delta_{ij}-\hat{R}_i\hat{R}_j)\}. \tag{3.7}$$

The addition of (3.7) to (3.6) through (3.5) extends the result to all post-overlap distances. Note that Ref. 58 displays an incorrect form of (3.7).

Work by Andrews and Juzeliūnas[79] added credence to the choice of contour above, deriving an identical result through inclusion of imaginary addenda in the form of the interaction Hamiltonian (2.7). The addenda effectively shift the poles away from the real axis so that a closed integration contour along the real axis necessarily encloses a pole in either the upper or lower imaginary plane. By choosing the anticlockwise, upper plane semicircle, (3.2) arises. Mathematically, however, there is no justification (only adoption of the outgoing wave condition) to preclude a clockwise semicircle which encloses the lower plane pole. In this respect, all results ultimately derived from the residue theorem reflect essentially classical ideas. This issue will be fully addressed in the following section where the quantum electrodynamical description of RET is rewritten, properly accounting for its key quantum mechanical effects.

B. New method

An alternative method for solving the integral of (2.19) entails a substitution expressing the result in terms of special functions. This technique avoids the use of contour integration in the complex plane which, as seen above, not only produces multiple answers but also has drawbacks in higher-order problems involving more than one virtual photon (where it can initially yield integrands without even symmetry).[80] As the new method can be applied to any integrand arising from a state-sequence diagram path, it proves a more durable alternative.

The Green's function (2.19) can be expressed as a sum of two integrals with the limits $p=[0,\infty]$

$$G(k,R)=\int_0^\infty \frac{\sin pR}{R(k-p)}dp+\int_0^\infty \frac{\sin pR}{R(-k-p)}dp. \tag{3.8}$$

Making the substitutions $t=pR-kR$ in the first integral and $s=pR+kR$ in the second gives

$$G(k,R)=-\frac{1}{R}\left(\int_{-kR}^\infty \frac{\sin(kR+t)}{t}dt+\int_{kR}^\infty \frac{\sin(-kR+s)}{s}ds\right). \tag{3.9}$$

Expansion of the numerators enables the integrands to be written solely as a function of the dummy variables, thus

$$G(k,R)=-\frac{1}{R}\left(\sin kR\int_{-kR}^\infty \frac{\cos t}{t}dt+\cos kR\int_{-kR}^\infty \frac{\sin t}{t}dt - \sin(kR)\int_{kR}^\infty \frac{\cos s}{s}ds+\cos(kR)\int_{kR}^\infty \frac{\sin s}{s}ds\right). \tag{3.10}$$

These integrals are expressible in terms of the cosine integral $\mathrm{Ci}(x)$ and the shifted sine integral $\mathrm{si}(x)$. These special functions, oscillatory with convergent amplitude, are defined as[81,82]

$$\mathrm{Ci}(x)=-\int_x^\infty \frac{\cos u}{u}du, \tag{3.11}$$

and

$$\mathrm{si}(x)=-\int_x^\infty \frac{\sin u}{u}du. \tag{3.12}$$

Note that as $x\to\infty$, $\mathrm{Ci}(x)=\mathrm{si}(x)\to 0$. Substituting (3.11) and (3.12) into Eq. (3.10) gives the requisite Green's function expressed as

$$G(k,R)=-\frac{\sin kR}{R}[\,\mathrm{Ci}(kR)-\mathrm{Ci}(-kR)] + \frac{\cos kR}{R}[\mathrm{si}(kR)+\mathrm{si}(-kR)]. \tag{3.13}$$

Noting that the shifted sine integral has the series expansion[81]

$$\mathrm{si}(x)=-\frac{\pi}{2}+\sum_{a=0}^\infty \frac{(-1)^a x^{2a+1}}{(2a+1)!(2a+1)}, \quad |x|<\infty, \tag{3.14}$$

it follows that

$$\mathrm{si}(x)+\mathrm{si}(-x)=-\pi. \tag{3.15}$$

Similarly, the cosine integral is also expressible in series form as

$$\mathrm{Ci}(x)=\gamma+\ln x+\sum_{a=1}^\infty \frac{(-1)^a x^{2a}}{(2a)!2a} \quad |\arg x|\leqslant\pi, \quad x<\infty, \tag{3.16}$$

where γ is Euler's constant, indicating that[81,83]

$$\mathrm{Ci}(-x\pm \mathrm{i}0)-\mathrm{Ci}(x)=\ln(-1)=\pm \mathrm{i}\pi, \tag{3.17}$$

where the infinite summations and γ conveniently cancel and the logarithm of a negative real number is taken as the Cauchy principal value. Inserting Eqs. (3.15) and (3.17) into (3.13) yields

$$G(k,R)=-\frac{\pi}{R}e^{\mp \mathrm{i}kR}, \tag{3.18}$$

which embraces the accepted result of (3.2) and also its complex conjugate, discarded in previous analyses.

The crux of this is that the outgoing wave approximation represents an untenable prejudice towards results of classical form—a device widely used by previous authors to bring a quantum model into line. The structure of (3.4) shows that the product of the donor transition moment and the interaction tensor, $\mu_i^{0\alpha(A)}V_{ij}(k,\mathbf{R})$, suggests a classical outgoing wave-vector field—though it is equally legitimate to regard the quantum amplitude as cast in terms of a product of the interaction tensor with the acceptor transition moment, $V_{ij}(k,\mathbf{R})\mu_j^{\beta 0(B)}$. However, $\mu_i^{0\alpha(A)}V_{ij}(k,\mathbf{R})$ represents a field which only approaches a transverse nature with respect to $\mathbf{R}$ in the long range $(kR\gg 1)$. In any other separation regime—and especially in the near-zone $(kR\ll 1)$, the field has components both transverse and longitudinal, as defined with respect to $\mathbf{R}$. One needs to recall that the virtual photon field (2.8) is precisely transverse with respect to the propagation vector $\mathbf{p}$—serving to emphasize that those photons are not confined to propagate directly from A to B.

After performing the necessary vector calculus a new, complete, form for the coupling tensor is given by

$$V_{ij}^{\pm}(k,\mathbf{R})=\frac{e^{\mp \mathrm{i}kR}}{4\pi\varepsilon_0 R^3}\{(1\pm \mathrm{i}kR)(\delta_{ij}-3\hat{R}_i\hat{R}_j) - k^2R^2(\delta_{ij}-\hat{R}_i\hat{R}_j)\}. \tag{3.19}$$

Commonly the negative sign is taken in (3.19), however both choices of sign are perfectly acceptable. It follows from (3.19) that its imaginary part

$$\tau_{ij}^{\pm}=(4\pi\varepsilon_0 R^3)^{-1}\{\mp(\sin kR-kR\cos kR)(\delta_{ij}-3\hat{R}_i\hat{R}_j) \pm k^2R^2\sin kR(\delta_{ij}-\hat{R}_i\hat{R}_j)\}, \tag{3.20}$$

displays the ambiguity in sign, whereas the real part of $V_{ij}^{\pm}(k,\mathbf{R})$ is identical to that given in (3.6). In passing we also note that the near-zone behavior of (3.19) mirrors that of Coulomb's law for an instantaneous interaction between transition electric dipoles, i.e., following R^{-3}. The ambiguities in the quantities $\mu_i^{0\alpha(A)}V_{ij}^{\pm}(k,\mathbf{R})$ and $V_{ij}^{\pm}(k,\mathbf{R})\mu_j^{\beta 0(B)}$ signify that $V_{ij}^{\pm}(k,\mathbf{R})$ describes both incoming and outgoing

waves—accommodating both state sequences (time orderings) as a correct quantum description should. It is important not to lose sight of the fact that $V_{ij}^{\pm}(k,\mathbf{R})$ is *part* of a quantum amplitude, a convenient construct but not a measurable. So long as the observable offers an accurate model of experimental data, then ambiguity at the quantum amplitude level is perfectly acceptable. This point is discussed further in Sec. V.

IV. ENERGY TRANSFER INVOLVING MAGNETIC-DIPOLE INTERACTIONS

The above discussion has focused on cases where the transitions of both donor and acceptor moieties are electric-dipole in character. However, magnetic-dipole interactions also need to be addressed. Their effect, usually observed only indirectly in interactions involving chiral species such as optical rotation,[84] circular dichroism[85] and circular differential scattering[86] is weak, and energy transfer processes are usually dominated by electric-dipole contributions. Here we develop the theory behind these interactions in light of the advances of Sec. III, and we offer circumstances where such interaction may dominate.

To examine the effects of magnetic-dipole interactions in resonance energy transfer we expand the interaction Hamiltonian introduced in Eq. (2.6) to include terms accommodating couplings of the donor and acceptor transitions with both electric and magnetic fields. Equation (2.7) is now

$$H_{\mathrm{int}}=-\sum_{\xi=A,B}\{\varepsilon_0^{-1}\boldsymbol{\mu}(\xi)\cdot\mathbf{d}^{\perp}(\mathbf{R}_{\xi})+\mathbf{m}(\xi)\cdot\mathbf{b}(\mathbf{R}_{\xi})\}, \quad (4.1)$$

which exhibits both the magnetic-dipole operator $\mathbf{m}(\xi)$ and the magnetic field operator $\mathbf{b}(\mathbf{R}_{\xi})$. The latter operator may again be expressed as a mode expansion—cf. (2.8),

$$\mathbf{b}(\mathbf{R}_{\xi})=\mathrm{i}\sum_{\mathbf{p},\lambda}\left(\frac{\hbar k}{2\varepsilon_0 cV}\right)^{\frac{1}{2}}\{\mathbf{b}^{(\lambda)}(\mathbf{p})a^{(\lambda)}(\mathbf{p})e^{\mathrm{i}\mathbf{p}\cdot\mathbf{R}_{\xi}} -\overline{\mathbf{b}}^{(\lambda)}(\mathbf{p})a^{\dagger(\lambda)}(\ \mathbf{p})e^{\mathrm{i}\mathbf{p}\cdot\mathbf{R}_{\xi}}\}, \quad (4.2)$$

where $\mathbf{b}^{(\lambda)}(\mathbf{p})$ is the polarization vector in the direction of the magnetic field vector and $\overline{\mathbf{b}}^{(\lambda)}(\mathbf{p})$ its complex conjugate. The incorporation of magnetic interactions into H_{int} increases the number of contributions to the quantum amplitude of RET. Alongside the pure electric-dipole–electric-dipole effect quantified by Eq. (3.3), both electric-dipole–magnetic-dipole $(e-m)$ and magnetic-dipole–magnetic-dipole $(m-m)$ couplings are included.

A slight modification of Fig. 1 accommodates the inclusion of magnetic-dipole interactions. Previously, connections between system-states indicated an application of the H_{int} given by (2.7), which only accounted for electric-dipole interactions. Here each interconnection must also entertain a magnetic-dipole interaction. As such the solid line paths in Fig. 3 represent the electric dipole coupling and the dotted line paths the magnetic counterpart. Contributions involving magnetic-dipole transitions both in the donor and the acceptor give negligible amplitude contributions and so can be discarded. As a result the cross-terms are the leading corrections accounting for magnetic-dipole influence.

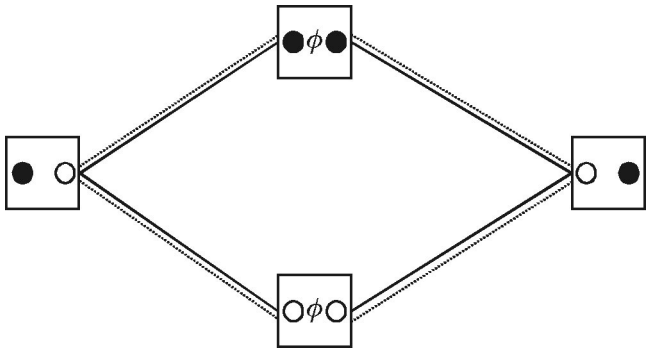

FIG. 3. Modified version of Fig. 1, solid and dotted lines depict electric and magnetic interactions, respectively.

Applying similar methods to those employed in the preceding section, the cross-term paths, which comprise a mixture of solid and dotted lines, are quantified by the quantum amplitudes $M_{fi}^{e-m}+M_{fi}^{m-e}$; we have two terms, the first where electric-dipole interactions occur at the donor and magnetic at the acceptor, and a second illustrating the converse. Explicitly

$$M_{fi}^{e-m}+M_{fi}^{m-e}=\frac{-\mathrm{i}k}{2\pi^2\varepsilon_0 c}\varepsilon_{ijk}\hat{R}_k\{\mu_i^{0\alpha(A)}m_j^{\beta 0(B)} +m_j^{0\alpha(A)}\mu_i^{\beta 0(B)}\}G'(k,R), \quad (4.3)$$

where the transition magnetic moment is given by $\mathbf{m}^{(r_k^m)'r_k^m(\xi)}=\langle\xi^{(r_k^m)'}|\mathbf{m}(\xi)|\xi^{r_k^m}\rangle$ and a new Green's function, $G'(k,R)$ is

$$G'(k,R)=\int_0^{\infty}\frac{1}{k^2-p^2}\left(\frac{p^2\cos pR}{R}-\frac{p\sin pR}{R^2}\right)dp. \quad (4.4)$$

The derivation of (4.3) utilizes a new polarization sum cast in terms of ε_{ijk}, the third-rank, antisymmetric Levi–Civita tensor,

$$\sum_{\lambda}e_i^{(\lambda)}(\mathbf{p})\overline{b}_l^{(\lambda)}(\mathbf{p})=\varepsilon_{jkl}\hat{p}_k(\delta_{il}-\hat{p}_i\hat{p}_l)=\varepsilon_{ijk}\hat{p}_k, \quad (4.5)$$

as follows from $\overline{\mathbf{b}}^{(\lambda)}(\mathbf{p})=\hat{\mathbf{p}}\times\overline{\mathbf{e}}^{(\lambda)}(\mathbf{p})$ and $\varepsilon_{jkl}\hat{p}_k\hat{p}_l=\hat{\mathbf{p}}\times\hat{\mathbf{p}}=0$. Also the identity

$$\frac{1}{4\pi}\int\hat{p}_k e^{\pm\mathrm{i}\mathbf{p}\cdot\mathbf{R}}d\Omega=\mp\mathrm{i}\left(\frac{\cos pR}{pR}-\frac{\sin pR}{p^2R^2}\right)\hat{R}_k \quad (4.6)$$

is used. Again, as in Sec. III, there are different methods of resolving the Green's function (4.4). Craig and Thirunamachandran used an integration contour identical to their solution of (2.19), offering[74]

$$G'(k,R)=\frac{\pi}{2R}(kR\cos kR+k^2R^2\sin kR) \quad (4.7)$$

which delivers the imaginary part of the total, all-space solution. This result was also derived in comprehensive RET work by Scholes *et al.*, which also included quadrupolar effects.[50] Each of the integration contours enumerated by Andrews and Sherborne can in fact be used to solve (4.4); how-

ever employing the new special functions method expedites an all-encompassing result by expressing (4.4) as

$$G'(k,R)=\frac{1}{2}\int_0^\infty\left(\frac{1}{-k-p}+\frac{1}{k-p}\right)\left(\frac{p\cos pR}{R}-\frac{\sin pR}{R^2}\right)dp. \tag{4.8}$$

The sine part of the integral is simply $-R^{-1}G(k,R)$, with its solution given by (3.18), thus

$$G'(k,R)=\frac{\pi}{2R^2}e^{\mp ikR}+\frac{1}{2R}\left(\int_0^\infty\frac{p\cos pR}{k-p}dp+\int_0^\infty\frac{p\cos pR}{-k-p}dp\right). \tag{4.9}$$

Making identical substitutions to those employed for (3.9) allows conversion to special functions as before; here, however, the process is not as straightforward. The Green's function is expressible as a sum of four integrals, thus

$$G'(k,R)=\frac{\pi}{2R^2}e^{\mp ikR}-\frac{1}{2R^2}\left\{\int_{-kR}^\infty\cos(t+kR)dt+kR\int_{-kR}^\infty\frac{\cos(t+kR)}{t}dt+\int_{kR}^\infty\cos(s-kR)ds-kR\int_{kR}^\infty\frac{\cos(s-kR)}{s}ds\right\} \tag{4.10}$$

with the second and fourth integrals performed as before. However the first and third terms exhibit nonconvergent amplitudes of oscillation obviating the use of special functions. Explicitly the first and third integrals produce

$$\int_{-kR}^\infty\cos(t+kR)dt+\int_{kR}^\infty\cos(s-kR)ds=\cos(kR)\left\{\int_0^\infty\cos t\,dt+\int_0^\infty\cos s\,ds\right\}, \tag{4.11}$$

which are solved by introducing a divergent exponential prefactor to each ($e^{-|\gamma|t}$ and $e^{-|\gamma|s}$, respectively). Using the general formula

$$\int_0^\infty e^{-ax}\cos bx dx=\frac{a}{a^2+b^2} \tag{4.12}$$

it can be verified that

$$\lim_{\gamma\to 0}\cos(kR)\left\{\int_0^\infty e^{-|\gamma|t}\cos t\,dt+\int_0^\infty e^{-|\gamma|s}\cos s\,ds\right\}=0. \tag{4.13}$$

Consequently,

$$G'(k,R)=\frac{\pi}{2R^2}e^{\mp ikR}-\frac{k}{2R}\{\cos(kR)[\mathrm{Ci}(kR)-\mathrm{Ci}(-kR)]+\sin(kR)[\mathrm{si}(-kR)+\mathrm{si}(kR)]\} \tag{4.14}$$

and, noting (3.15) and (3.17), the evaluation can be completed to yield

$$G'(k,R)=\frac{\pi e^{\mp ikR}}{2R^2}(1\pm ikR) \tag{4.15}$$

(associated with the use of contours C_3 and C_4). Using (4.15), the quantum amplitude can be written as

$$M_{fi}^{e-m}+M_{fi}^{m-e}=\left\{\mu_i^{0\alpha(A)}\frac{m_j^{\beta 0(B)}}{c}+\frac{m_j^{0\alpha(A)}}{c}\mu_i^{\beta 0(B)}\right\}U_{ij}^{\pm}(k,\mathbf{R}) \tag{4.16}$$

which features the fully retarded electric-dipole–magnetic-dipole interaction tensor, expressed as

$$U_{ij}^{\pm}(k,\mathbf{R})=\rho_{ij}^{\pm}+i\vartheta_{ij}, \tag{4.17}$$

echoing (3.5). As stated previously, Ref. 74 gives only the imaginary part, explicitly

$$\vartheta_{ij}=\frac{\varepsilon_{ijk}}{4\pi\varepsilon_0}\frac{\hat{R}_k}{R^3}(-kR\cos kR-k^2R^2\sin kR), \tag{4.18}$$

whereas our method reveals an additional real part

$$\rho_{ij}^{\pm}=\frac{\varepsilon_{ijk}}{4\pi\varepsilon_0}\frac{\hat{R}_k}{R^3}(\mp kR\sin kR\pm k^2R^2\cos kR). \tag{4.19}$$

Adding (4.18) and (4.19) gives the total expression for $U_{ij}^{\pm}(k,\mathbf{R})$ as the following second-rank, antisymmetric tensor:

$$U_{ij}^{\pm}(k,\mathbf{R})=\frac{e^{\mp ikR}}{4\pi\varepsilon_0}\varepsilon_{ijk}\frac{\hat{R}_k}{R^3}(-ikR\pm k^2R^2). \tag{4.20}$$

To expedite the comparisons undertaken in the following section, both $U_{ij}^{\pm}(k,\mathbf{R})$ and $V_{ij}^{\pm}(k,\mathbf{R})$ are cast in the same units, as with $\boldsymbol{\mu}$ and $\mathbf{m}/c$ [c has been included in other versions of the coupling tensor $U_{ij}^{\pm}(k,\mathbf{R})$ in some previous analyses]. Also note that there is no R^{-3} term in (4.20) indicating that, in the near-zone limit, any electric-dipole interactions will overwhelmingly dominate. Furthermore (4.20) affords insight into why static electric- and magnetic-dipoles do not interact; in the static limit of $k=0$, (4.20) is zero.

V. RATE EQUATIONS AND DISCUSSION

An observable for the process of resonance energy transfer (in this case a rate, Γ) is calculated by use of the Fermi golden rule,[87]

$$\Gamma=\frac{2\pi}{\hbar}|M_{fi}|^2\rho_f, \tag{5.1}$$

where ρ_f is the density of acceptor final states. The overall transfer quantum amplitude M_{fi},

$$M_{fi}=M_{fi}^{e-e}+M_{fi}^{e-m}+M_{fi}^{m-e}+M_{fi}^{m-m}, \tag{5.2}$$

thus comprises a sum of the contributions from electric and magnetic interactions.

A. Selection rules

First we note that, in order for all the terms in (5.2) to contribute, it is necessary that the donor decay transition

$|0\rangle \leftarrow |\alpha\rangle$ is both electric-dipole and magnetic-dipole allowed. This is a criterion that is invariably satisfied when A is chiral but is not met when A is centrosymmetric. For donor molecules which are neither chiral nor centrosymmetric, each case is determined by the symmetry of the transition. Similar remarks apply to the excitation transition $|\beta\rangle \leftarrow |0\rangle$ in the acceptor molecule B. Thus it is possible for situations to arise where the selection rules dictate that only one of the components in (5.2) is nonzero. Although purely magnetic energy transfer is generally a negligible contributor, its quantum amplitude, the fourth term in (5.2), can result in significant interference terms—especially with the purely electric quantum amplitude, the first term.[88] However in the analysis which follows, systems will be envisaged in which this specific interference is precluded.

B. Rotationally averaged rates

Disregarding this fourth term in the quantum amplitude, we have a maximum of nine rate contributions to be addressed. First, assuming that both the donor and acceptor transitions are electric-dipole allowed, the pure electric-dipole–electric-dipole contribution is given by

$$M_{fi}^{e-e}\overline{M}_{fi}^{e-e} = |\boldsymbol{\mu}^A|^2|\boldsymbol{\mu}^B|^2 A(k,R), \tag{5.3}$$

after appropriate second-rank rotational averaging methods have been applied.[89] Equation (5.3) introduces the shorthand notation $|\boldsymbol{\mu}^{0\alpha(A)}| \equiv |\boldsymbol{\mu}^A|$, $|\boldsymbol{\mu}^{\beta 0(B)}| \equiv |\boldsymbol{\mu}^B|$. Also present is the $e-e$ excitation transfer function $A(k,R)$ given by;

$$\begin{aligned} A(k,R) &= V_{ij}^{\pm}(k,\mathbf{R})\overline{V}_{ij}^{\pm}(k,\mathbf{R}) \\ &= \frac{2}{(4\pi\varepsilon_0 R^3)^2}(3+k^2R^2+k^4R^4), \end{aligned} \tag{5.4}$$

a scalar field characterizing the $e-e$ unified mechanism (note the short-range R^{-6} and long-range R^{-2} dependencies—*vide infra*). Importantly, $A(k,R)$ carries no ambiguity in sign. The new technique not only correctly describes the proper quantum behavior of RET but also delivers a physically unambiguous and observable description of the rate.

Four quantum interference terms in (5.1) are the products $M_{fi}^{e-e}\overline{M}_{fi}^{e-m}$ and $M_{fi}^{e-e}\overline{M}_{fi}^{m-e}$ and their complex conjugates. The contribution from each of these terms disappears as each contains either $V_{ij}^{\pm}(k,\mathbf{R})\overline{U}_{ij}^{\pm}(k,\mathbf{R})$ or its complex conjugate, leading to the tensor contractions $\varepsilon_{ijk}\delta_{ij}\hat{R}_k$ and $\varepsilon_{ijk}\hat{R}_i\hat{R}_j\hat{R}_k$, each of which is zero. That this quantum interference term is null indicates that the two types of energy transfer ($e-e$ and $e-m$) described above do not mix on a quantum level. Henceforth we may think of the rate potentially comprising contributions from pure $e-e$, pure $e-m$, or pure $m-e$ transfer, and this proves fruitful for the ensuing discussion.

The rate contributions emerging from the electric-dipole–magnetic-dipole terms, again after second-rank averaging, are given by

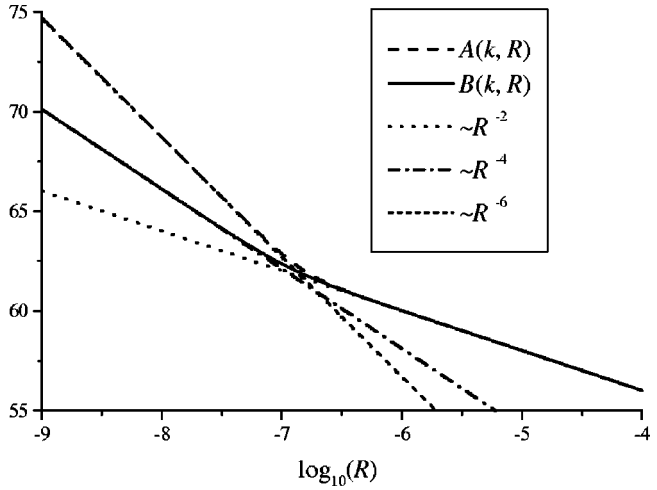

FIG. 4. Log–log plot illustrating values for A^{SR} and B^{SR}, over appropriate transfer distances R: $k=9\times10^6$ m^{-1}.

$$\begin{aligned} |M_{fi}^{e-m}+M_{fi}^{m-e}|^2 = \frac{B(k,R)}{9c^2}\{&|\boldsymbol{\mu}^A|^2|\mathbf{m}^B|^2 \\ &+|\boldsymbol{\mu}^B|^2|\mathbf{m}^A|^2-2\Re|\boldsymbol{\mu}^A\cdot\overline{\mathbf{m}}^A||\overline{\boldsymbol{\mu}}^B\cdot\mathbf{m}^B|\}, \end{aligned} \tag{5.5}$$

where $|\mathbf{m}^{0\alpha(A)}| \equiv |\mathbf{m}^A|$, $|\mathbf{m}^{\beta 0(B)}| \equiv |\mathbf{m}^B|$. In a similar manner to (5.3) these contributions are dictated by a new scalar field dependent on k and R, the $e-m$ excitation transfer function $B(k,R)$ explicitly written as

$$\begin{aligned} B(k,R) &= U_{ij}^{\pm}(k,\mathbf{R})\overline{U}_{ij}^{\pm}(k,\mathbf{R}) \\ &= -U_{ij}^{\pm}(k,\mathbf{R})\overline{U}_{ji}^{\pm}(k,\mathbf{R}) \\ &= \frac{2}{(4\pi\varepsilon_0 R^3)^2}(k^2R^2+k^4R^4). \end{aligned} \tag{5.6}$$

In contrast to its $e-e$ analogue, $B(k,R)$ lacks an R^{-6} term—meaning that, in the near-zone where coupling is strongest, electric-magnetic interactions offer only a small correction if $e-e$ coupling is allowed. Comparison of (5.3) and (5.5) highlights major differences between the overall rate contributions associated with the two mechanisms. A typical transition dipole moment is of the order of 1D, two or three orders of magnitudes larger than $|\mathbf{m}^{\xi}|/c$ when $|\mathbf{m}^{\xi}| = 1\,\mu_B$. Thus each substitution of $|\boldsymbol{\mu}^{\xi}|$ with $|\mathbf{m}^{\xi}|/c$, essentially the replacement of a dipole interaction with a magnetic one, reduces the overall rate contribution of $e-m$ terms by a factor of between 100 and 1000, even before taking into account the comparative forms of $A(k,R)$ and $B(k,R)$. For the latter comparison, however, it is interesting to measure the two transfer functions against each other over appropriate distance regimes. Assuming absorption of light at 700 nm, giving $k=9\times10^6$ m^{-1}, the responses of $A(k,R)$ and $B(k,R)$ over distances between 1 nm and 10 μm are plotted in Fig. 4.

From Fig. 4 it can be seen that the functions $A(k,R)$ and $B(k,R)$ converge in the long-range limit $kR \gg 1$. Applying this to (5.3) and (5.6) reveals that

$$A^{\mathrm{LR}}(k,R)=B^{\mathrm{LR}}(k,R)=\frac{2k^4}{(4\pi\varepsilon_0 R)^2}, \tag{5.7}$$

where the superscript LR indicates the long-range limit. Necessarily, long-range inverse square law behavior emerges; Eq. (5.7) indicates that it is only the comparative strengths of $|\boldsymbol{\mu}^{\xi}|$ and $|\mathbf{m}^{\xi}|/c$ which are important in determining the relative significance of $e-e$ and $e-m$ $(m-e)$ coupling in the wave zone. Conversely in the short-range limit $(kR\ll 1)$ the $e-e$ transfer function is given by

$$A^{\mathrm{SR}}(k,R)=\frac{6}{(4\pi\varepsilon_0 R^3)^2}, \tag{5.8}$$

and the $e-m$ analogue is

$$B^{\mathrm{SR}}(k,R)=\frac{2k^2}{(4\pi\varepsilon_0 R^2)^2}. \tag{5.9}$$

The ratio of A^{SR} to B^{SR} over a short-range regime is $3/k^2\,R^2$ which, between 10 Å and 100 Å varies from $\sim 10^4$ to $\sim 10^2$ (again using $k=9\times 10^6\ \mathrm{m}^{-1}$). This further reinforces $e-e$ dominance for Förster-zone transfer—even before taking into account the relative magnitudes of $|\boldsymbol{\mu}^{\xi}|$ and $|\mathbf{m}^{\xi}|/c$.

C. Ordered systems

As has been established above, if the donor and acceptor species involved in energy transfer undergo one-photon transitions which are both magnetic- and electric-dipole allowed, the $e-m$ and $m-e$ energy transfer mechanisms are generally of little consequence as the $e-e$ term dominates—the other terms offering, at best, a small adjustment to the overall rate for fluid media. However, ordered systems can be envisaged in which the mutual orientation of the transfer pair itself forbids $e-e$ transfer, irrespective of the selection rules.

Concentrating on the short-range results, the rate of energy transfer can be expressed in terms of an orientation factor κ as commonly reported in the literature.[90,91] Assuming real transition electric-dipole moments,

$$|M_{fi}^{e-e}\overline{M}_{fi}^{e-e}|^2=\frac{|\boldsymbol{\mu}^A|^2|\boldsymbol{\mu}^B|^2\kappa^2}{16\pi^2\varepsilon_0^2 R^6}, \tag{5.10}$$

where

$$\kappa=\cos\theta-3\cos\phi\cos\gamma. \tag{5.11}$$

The orientation factor is expressed by three angles—θ the angle between $|\boldsymbol{\mu}^A|$ and $|\boldsymbol{\mu}^B|$, and ϕ and γ the angles between $\hat{\mathbf{R}}$ and $|\boldsymbol{\mu}^A|$ and $|\boldsymbol{\mu}^B|$, respectively. It is obvious that, when the vectors involved form an orthogonal triad, κ (and hence the rate contribution of $e-e$ transfer) is zero. It has however been shown that, in certain spirane-based systems, vibrational effects can break the symmetry and hence facilitate energy transfer.[92] Then, $e-e$ transfer still dominates the rate, as shown by the picosecond measurements reported in Ref. 92. Nonetheless, where such vibrational symmetry-lowering is absent, energy transfer may still proceed through a coupling described by the leading electric–magnetic interference contributions, which follow from (4.16) and (4.20). Expressing the result in terms of vector triple products, in the short-range the rate counterpart to (5.10) is as follows:

$$|M_{fi}^{e-m}+M_{fi}^{m-e}|^2=\frac{k^2}{4\pi^2c^2\varepsilon_0^2R^4}\{\hat{\mathbf{R}}\cdot(\boldsymbol{\mu}^A\times\mathbf{m}^B)+\hat{\mathbf{R}}\cdot(\mathbf{m}^A\times\boldsymbol{\mu}^B)\}^2. \tag{5.12}$$

If, for example, *within each species* (A or B) the magnetic- and electric-dipole transition moments are collinear, then, if the transition dipoles and intermolecular vector form an orthogonal triad, we automatically preclude pure $e-e$ transfer leaving (5.12) as the leading term. Thus

$$|M_{fi}^{e-m}+M_{fi}^{m-e}|^2=\frac{k^2|\boldsymbol{\mu}^A|^2|\boldsymbol{\mu}^B|^2}{4\pi^2\varepsilon_0^2R^4}(C_A+C_B)^2, \tag{5.13}$$

where $C_{\xi}|\boldsymbol{\mu}^{\xi}|=|\mathbf{m}^{\xi}|/c$ and Θ is the angle between $\hat{\mathbf{R}}$ and the normal to both the $\boldsymbol{\mu}^A\mathbf{m}^B$ plane and $\boldsymbol{\mu}^B\mathbf{m}^A$ plane. The result (5.13) shows that it is possible to elicit a response for energy transfer driven by electric–magnetic coupling when $e-e$ transfer is forbidden. Such geometric interaction-pair control might, for example, be achieved in a suitably nonsymmetric bichromophore system or a layered Langmuir–Blodgett film.

To conclude we note that, compared to the usual electric–electric coupling mechanism, energy transfer mediated by electric–magnetic coupling is extremely weak, being associated with rates several orders of magnitude smaller. However, in systems where $e-e$ coupling is precluded (either by selection rules or by geometric arrangement) it is possible to envisage experiments based on ultrasensitive fluorescence detection that will, for the first time, enable the direct detection of $e-m$ mechanisms.

ACKNOWLEDGMENTS

The authors wish to thank E. A. Power and T. Thirunamachandran for helpful and insightful comments on the paper. We also acknowledge the Engineering and Physical Sciences Research Council for funding this work.

[1] A. A. Demidov and A. Yu. Borisov, Biophys. J. **64**, 1375 (1993).
[2] R. van Grondelle, J. Dekker, T. Gillbro, and V. Sundström, Biochim. Biophys. Acta **1187**, 1 (1994).
[3] K. Schulten, in *Simplicity and Complexity in Proteins and Nucleic Acids*, edited by H. Frauenfelder, J. Deisenhofer, and P. G. Wolynes (Dahlem University Press, Berlin 1999), pp. 227–253.
[4] T. Markvart, Prog. Quantum Electron. **24**, 107 (2000).
[5] T. Renger, V. May, and O. Kühn, Phys. Rep. **343**, 137 (2001).
[6] J. Deisenhofer, O. Epp, K. Miki, R. Huber, and H. Michel, Nature (London) **318**, 618 (1985).
[7] G. McDermott, S. M. Prince, A. A. Freer, A. M. Hawthornthwaite-Lawless, M. Z. Papiz, R. J. Cogdell, and N. W. Isaacs, Nature (London) **374**, 517 (1995).
[8] V. Sundström, T. Pullerits, and R. van Grondelle, J. Phys. Chem. B **103**, 2327 (1999).
[9] R. E. Fenna and B. C. Matthews, Nature (London) **258**, 573 (1975).
[10] W. Kühlbrandt and D. N. Wang, Nature (London) **350**, 130 (1991).
[11] W. Kühlbrandt, D. N. Wang, and Y. Fujiyoshi, Nature (London) **367**, 614 (1994).
[12] N. Krauss, W.-D. Schubert, O. Klukas, P. Fromme, H. T. Witt, and W. Saenger, Nat. Struct. Biol. **3**, 965 (1996).
[13] M. Maus, R. De, M. Lor, T. Weil, S. Mitra, U.-M. Wiesler, A. Herrmann,

J. Hofkens, T. Vosch, K. Müllen, and F. C. De Schryver, J. Am. Chem. Soc. **123**, 7668 (2001).
[14] J.-S. Hsiao, B. P. Krueger, R. W. Wagner, T. E. Johnson, J. K. Delaney, D. C. Mauzerall, G. R. Fleming, J. S. Lindsey, D. F. Bocian, and R. J. Donohoe, J. Am. Chem. Soc. **118**, 11181 (1996).
[15] D. M. Guldi, Chem. Soc. Rev. **31**, 22 (2002).
[16] D. Kuciauskas, P. A. Liddell, S. Lin, T. E. Johnson, S. J. Weghorn, J. S. Lindsey, A. L. Moore, T. A. Moore, and D. Gust, J. Am. Chem. Soc. **121**, 8604 (1999).
[17] F. C. De Schryver, N. Boens, and J. Put, Adv. Photochem. **10**, 359 (1977).
[18] S. Speiser, J. Photochem. **22**, 195 (1983).
[19] B. Valeur, in *Fluorescent Biomolecules: Methodologies and Applications*, edited by D. M. Jameson and G. D. Reinhardt (Plenum Press, New York, 1989), pp. 269–303.
[20] M. N. Berberan-Santos, J. Pouget, B. Valeur, J. Canceill, L. Jullien, and J.-M. Lehn, J. Phys. Chem. **97**, 11376 (1993).
[21] M. N. Berberan-Santos, P. Choppinet, A. Fedorov, L. Jullien, and B. Valeur, J. Am. Chem. Soc. **121**, 2526 (1999).
[22] P. G. Van Patten, A. P. Shreve, J. S. Lindsey, and R. J. Donohoe, J. Phys. Chem. B **102**, 4209 (1998).
[23] P. Brodard, S. Matzinger, E. Vauthey, O. Mongin, C. Papamicaël, and A. Gossauer, J. Phys. Chem. A **103**, 5858 (1999).
[24] R. K. Lammi, R. W. Wagner, A. Ambrose, J. R. Diers, D. F. Bocian, D. Holten, and J. S. Lindsey, J. Phys. Chem. B **105**, 5341 (2001).
[25] A. Archut and F. Vögtle, Chem. Soc. Rev. **27**, 233 (1998).
[26] C. Devadoss, P. Bharathi, and J. S. Moore, J. Am. Chem. Soc. **118**, 9635 (1996).
[27] D. M. Junge and D. V. McGrath, Chem. Commun. **1997**, 857.
[28] D.-L. Jiang and T. Aida, Nature (London) **388**, 454 (1997).
[29] A. Bar-Haim, J. Klafter, and R. Kopelman, J. Am. Chem. Soc. **119**, 6197 (1997).
[30] A. Adronov and M. J. Fréchet, Chem. Commun. **2000**, 1701.
[31] M. R. Shortreed, S. F. Swallen, Z.-Y. Shi, W. Tan, Z. Xu, C. Devadoss, J. S. Moore, and R. Kopelman, J. Phys. Chem. B **101**, 6318 (1997).
[32] R. D. Jenkins and D. L. Andrews, J. Chem. Phys. **118**, 3470 (2003).
[33] L. Stryer, Annu. Rev. Biochem. **47**, 819 (1978).
[34] P. R. Selvin, Method Enzymol. **246**, 300 (1995).
[35] S. Arnold, S. Holler, and S. D. Druger, J. Chem. Phys. **104**, 7741 (1996).
[36] V. V. Ovsyankin, in *Spectroscopy of Solids Containing Rare Earth Ions*, edited by A. A. Kaplyanskii and R. M. Macfarlane (Elsevier, Amsterdam, 1987), pp. 343–481.
[37] A. Ruseckas, M. Theander, L. Valkunas, M. R. Andersson, O. Inganäs, and V. Sundström, J. Lumin. **76–77**, 474 (1998).
[38] K. Sienicki, J. Chem. Phys. **94**, 617 (1991).
[39] A. Murphy, F. Grieser, D. Y. C. Chan, D. N. Furlong, and B. Mathews, Colloids Surf., A **102**, 1 (1995).
[40] E. Vuorimaa, H. Lemmetyinen, P. Ballet, M. Van der Auweraer, and F. C. De Schryver, Langmuir **13**, 3009 (1997).
[41] S. Woutersen and H. J. Bakker, Nature (London) **402**, 507 (1999).
[42] H. Kuhn and D. Möbius, Angew. Chem., Int. Ed. Engl. **10**, 620 (1971).
[43] B. Richter and S. Kirstein, J. Chem. Phys. **111**, 5191 (1999).
[44] I. Yamazaki, N. Tamai, and T. Yamazaki, J. Phys. Chem. **94**, 516 (1990).
[45] D. C. Saha, D. Bhattacharjee, and T. N. Misra, Opt. Mater. **10**, 285 (1998).
[46] Z. Zhang, A. L. Verma, K. Nakashima, M. Yoneyama K. Iriyama, and Y. Ozaki, Langmuir **13**, 5726 (1997).
[47] Z.-J. Zhang, A. L. Verma, K. Nakashima, K. Iriyama, and Y. Ozaki, Thin Solid Films **333**, 1 (1998).
[48] M. L. Grayeski and P. A. Moritzen, Langmuir **13**, 2675 (1997).
[49] D. L. Dexter, J. Chem. Phys. **21**, 836 (1953).
[50] G. D. Scholes, A. H. A. Clayton, and K. P. Ghiggino, J. Chem. Phys. **97**, 7405 (1992).
[51] G. D. Scholes and K. P. Ghiggino, J. Chem. Phys. **101**, 1251 (1994).
[52] R. D. Harcourt, G. D. Scholes, and K. P. Ghiggino, J. Chem. Phys. **101**, 10521 (1994).
[53] G. D. Scholes, R. D. Harcourt, and K. P. Ghiggino, J. Chem. Phys. **102**, 9574 (1995).
[54] G. D. Scholes and K. P. Ghiggino, J. Chem. Phys. **103**, 8873 (1995).
[55] T. Förster, Ann. Phys. (Paris) **6**, 55 (1948).
[56] J. S. Avery, Proc. Phys. Soc. London **88**, 1 (1966).
[57] M. N. Berberan-Santos, E. J. Nunes Pereira, and J. M. G. Martinho, in *Resonance Energy Transfer*, edited by D. L. Andrews and A. A. Demidov (Wiley, Chichester, 1999), pp. 108–149.
[58] D. L. Andrews and B. S. Sherborne, J. Chem. Phys. **86**, 4011 (1987).
[59] D. L. Andrews, Chem. Phys. **135**, 195 (1989).
[60] G. D. Scholes and D. L. Andrews, J. Chem. Phys. **107**, 5374 (1997).
[61] L. Gomberoff and E. A. Power, Proc. Phys. Soc. London **88**, 281 (1966).
[62] R. P. Feynman, *Quantum Electrodynamics* (W. A. Benjamin, New York, 1962).
[63] F. Halzen and A. D. Martin, *Quarks and Leptons* (Wiley, New York, 1984), p. 140.
[64] R. D. Jenkins and D. L. Andrews, J. Chem. Phys. **116**, 6713 (2002).
[65] R. D. Jenkins, D. L. Andrews, and L. C. Dávila Romero, J. Phys. B **35**, 445 (2002).
[66] D. P. Craig and T. Thirunamachandran, Chem. Phys. **167**, 229 (1992).
[67] E. A. Power and T. Thirunamachandran, Phys. Rev. A **56**, 3395 (1997).
[68] R. D. Jenkins, G. J. Daniels, and D. L. Andrews (unpublished).
[69] J. Knoester and S. Mukamel, Phys. Rev. A **40**, 7065 (1989).
[70] G. Juzeliūnas and D. L. Andrews, Phys. Rev. B **49**, 8751 (1994).
[71] G. Juzeliūnas and D. L. Andrews, Phys. Rev. B **50**, 13371 (1994).
[72] P. W. Milonni, J. Mod. Opt. **42**, 1991 (1995).
[73] G. Juzeliūnas and D. L. Andrews, in *Resonance Energy Transfer*, edited by D. L. Andrews and A. A. Demidov (Wiley, Chichester, 1999) pp. 65–107.
[74] D. P. Craig and T. Thirunamachandran, *Molecular Quantum Electrodynamics* (Dover, Mineola, NY, 1998).
[75] P. M. Morse and H. Feshbach, *Methods of Theoretical Physics Part 1* (McGraw-Hill, New York, 1953).
[76] G. Barton, *Elements of Green's Functions and Propagation* (Oxford University Press, New York, 1989).
[77] J. D. Jackson, *Classical Electrodynamics*, 2nd ed. (Wiley, New York, 1975).
[78] D. P. Craig and T. Thirunamachandran, Adv. Quantum Chem. **16**, 97 (1982).
[79] D. L. Andrews and G. Juzeliūnas, J. Chem. Phys. **96**, 6606 (1992).
[80] G. J. Daniels, R. D. Jenkins, and D. L. Andrews (unpublished).
[81] N. N. Lebedev, *Special Functions and their Applications* (Prentice-Hall, New Jersey, 1965).
[82] L. C. Andrews, *Special Functions of Mathematics for Engineers*, 2nd ed. (Oxford University Press, Oxford, 1992).
[83] E. W. Weisstein, *CRC Concise Encyclopaedia of Mathematics*, 2nd ed. (Chapman and Hall/CRC, Boca Raton, FL, 2003), p. 1989.
[84] E. A. Power and T. Thirunamachandran, J. Chem. Phys. **55**, 5322 (1971).
[85] E. A. Power and T. Thirunamachandran, J. Chem. Phys. **60**, 3695 (1974).
[86] D. L. Andrews, J. Chem. Phys. **72**, 4141 (1980).
[87] P. A. M. Dirac, *Principles of Quantum Mechanics* (Oxford University Press, Oxford, 1967).
[88] D. P. Craig and T. Thirunamachandran, J. Chem. Phys. **109**, 1259 (1998).
[89] D. L. Andrews and M. J. Harlow, Phys. Rev. A **29**, 2796 (1984).
[90] B. W. van der Meer, in *Resonance Energy Transfer*, edited by D. L. Andrews and A. A. Demidov (Wiley, Chichester, 1999), pp. 151–172.
[91] B. W. van der Meer, Mol. Biotechnol. **82**, 181 (2002).
[92] W. T. Yip, D. H. Levy, R. Kobetic, and P. Piotrowiak, J. Phys. Chem. A **103**, 10 (1999).